CrossMark

Effect of welan gum on the hydration and hardening of Portland cement

Yu Zhang[1,2] · Zuhua Zhang[3,4] · Xuerun Li[5] · Weifeng Li[1] · Xiaodong Shen[1,2] · Hao Wang[3,4]

Abstract This paper reports the effects of welan gum on the hydration and hardening behaviors of Portland cement (PC) by using X-ray diffractometry, mercury instruction porosimetry, thermogravimetry, differential scanning calorimetry and scanning electron microscopy. Results show that welan gum has notable influence on the setting time of PC paste and the formation of calcium hydroxide $(Ca(OH)_2)$; welan gum has little impact on the total hydration heat, AFt content and/or the morphologies of hydration products even though it delays the induction period of hydration and the second reaction of the aluminate phase. Welan gum retards the early hydration of C_3S and accelerates the early hydration of C_4AF. The compressive strength is improved, and pore size of hardened cement paste is reduced with at the studied period when welan gum is no more than 0.05%. In this research, the cement paste with 0.05% welan gum exhibits the highest long-term (90 d) compressive strength and lowest porosity.

✉ Yu Zhang
 zhangyuzeus@163.com

✉ Xiaodong Shen
 xdshen@njtech.edu.cn

1 State Key Laboratory of Materials-Oriented Chemical Engineering, College of Materials Science and Engineering, Nanjing Tech University, No. 5 Xin Mofan Road, Nanjing 210009, People's Republic of China

2 Jiangsu National Synergetic Innovation Center for Advanced Materials (SICAM), Nanjing 210009, People's Republic of China

3 China-Australia Institute for Advanced Materials and Manufacturing, Jiaxing University, Jiaxing 314001, China

4 Centre for Future Materials, University of Southern Queensland, Toowoomba, QLD 4350, Australia

5 Laboratory of Construction Materials, Ecole Polytechnique Fédérale de Lausanne (EPFL), 1015 Lausanne, Switzerland
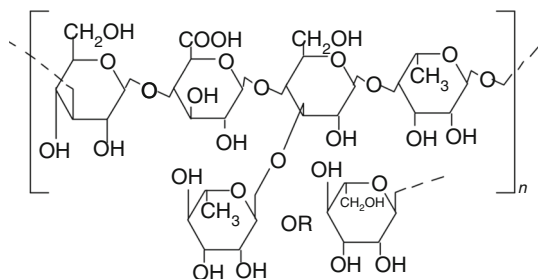
Introduction

Welan gum is high molecular microbial polysaccharides produced by the fermentation of Alcaligenes species and has been widely used in food production, petroleum industry, medical production and in various other fields [1–5]. It is also used in cementitious materials due to the excellent properties in thickening and controlling separation [6–8], which are used in underwater repair of marine structures, deep foundation walls and some tremie concrete constructions [1, 9]. Researchers [7, 10–12] have reported the favorable effect of welan gum on the rheology of cement grout that can be used to adjust the workability and improve water retention capacity, so it is also used in the preparation of self-consolidating concrete [13, 14]. Welan gum is also temperature insensitive (it maintains viscosity at temperature as high as 149 °C) [15, 16], which confirms the application in large volume concrete where temperature rises due to hydration heat occurs. The molecular structure of welan gum is shown in Fig. 1.

In the past three decades, the effect of welan gum on rheology of concrete, mortar and cement grout has been studied [1, 2, 10, 17, 18]. A few studies on the effect of welan gum addition on the hydration of minerals of cement clinker were reported [19, 20]. Ma et al. [19] pointed out that welan gum postponed the initial formation of ettringite in the tricalcium aluminate (C_3A)[1]–gypsum system

---

1 Cement nomenclature will be used, i.e., C = CaO, S = SiO$_2$, A = Al$_2$O$_3$, F = Fe$_2$O$_3$, \$ = SO$_3$, H = H$_2$O.

Fig. 1 Molecular structure of welan gum

Table 1 Chemical and mineral compositions of PII 52.5 cement (mass%)

Oxide		Mineral composition	
CaO	64.8	C_3S	59.4
SiO_2	18.8	C_2S	13.8
Al_2O_3	4.1	C_4AF	9.4
Fe_2O_3	3.9	C_3A	6.5
SO_3	2.9	Calcite	4.8
MgO	0.7	Gypsum	2.6
K_2O	0.7	Bassanite	1.6
Na_2O	0.1	Anhydrite	0.7
Loss on ignition	3.20	f-CaO	0.4
		Periclase	0.8

because it hindered the nucleation and growth of ettringite. The authors supposed that the welan gum molecules locked the SO_4^{2-} and decreased the hydration activity of adsorbed regions; therefore, the ettringite could not cover the surface of C_3A. As a consequence, the hydration process was delayed. Zhang et al. [20] found that welan gum could retard the early hydration of C_3S and hinder the precipitation of $Ca(OH)_2$ on C_3S surface; however, welan gum has no influence on the nucleation of $Ca(OH)_2$ and does not change the orientation distribution of hydration products.

Even though the previous researchers have achieved great success during the studying the effects of welan gum on the hydration of mono-minerals [19, 20], the interaction effect of these components in cements in the presence of welan gum is unclear. To date, there is very limited attention paid to the effect of welan gum on the hydration of Portland cement (PC). An in-depth understanding of the effects of welan gum on the hydration and the optimum dosage in utilization will be critically useful and necessary for the application of welan gum. In this paper, six concentrations of welan gum solutions were used to study the effect of welan gum on the hydration and hardening properties to seek a good understanding of welan gum in cement system and provide a way for the practical use of welan gum.

Experimental

Materials

Grinding aid-free PII 52.5-grade cement from Jiangnan Xiaoyetian Cement Manufacturer was used to avoid any potential influence of grinding aid on the hydration. It has a fineness of 367 $m^2\ kg^{-1}$ (Blaine). X-ray fluorescence (XRF) and Rietveld quantitative X-ray diffraction (XRD) analyses were performed on the cement, and the results are given in Table 1. According to the results, silicate phases make up to over 72% of the cement minerals and alkalis are at low level. Particle size distribution as determined by Microtrac S3500 is shown in Fig. 2. D_{50} of the cement is 18.14 μm.
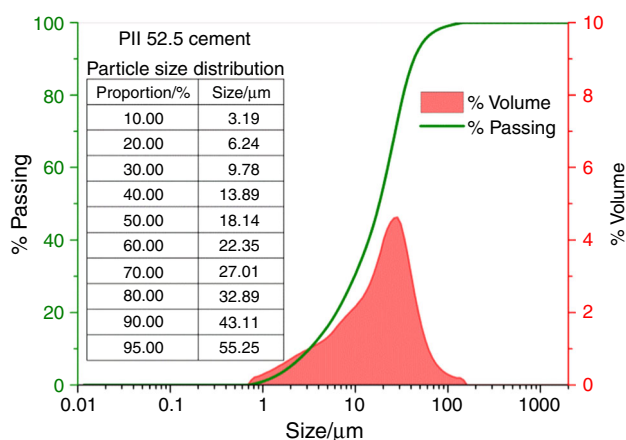

Fig. 2 Particle size distribution of PII 52.5 cement

The welan gum used in this study was bought from Hebei Henbo Biotechnology Co., Ltd. (Xinhe, Hebei Province, China). Six concentrations of welan gum solutions were prepared for the use of cement mixing: 0.00% (blank), 0.025% (the mass ratios to water), 0.05, 0.075, 0.10 and 0.25%. All of solutions were well mixed and stored at 20 °C.

Methods and characterization

Setting time

Cement pastes for setting time tests were prepared according to the water requirement for normal consistency according to Chinese National Standard (GB/T 1346-2001). For each solution, the water requirement must be determined before measuring setting time.

Compressive strength testing

Compressive strength testing was performed using standard mortars prepared with cement:sand:welan gum

solution = 1:3:0.5. The sample preparation and testing procedure were according to the Chinese National Standard (GB/T17671-1999, similar to ISO 679). Prismatic samples (40 × 40 × 160 mm) were cured at 20 ± 1 °C and relative humidity (RH) 95%. After 1 d of hardening, samples were demolded and immersed in water (20 ± 1 °C) until testing at 1, 3, 28 and 90 d using a universal mechanical testing machine at a loading rate of 1.5 ± 0.1 MPa s^{-1}. At least 3 specimens (6 compressive strength values) were tested for each mix and the mean values reported with the standard deviations as apparent errors.

Hydration characterization

To investigate the hydration process, isothermal calorimetry (at 20 °C) was performed over the first 90 h of hydration, using 6 g of paste with a solution/cement (w/c) of 0.5 was placed in a plastic ampoule and heat evolution was recorded using an eight-channel TAM air isothermal calorimeter. The w/c ratio and curing temperature were kept constant during the experiment as they both have significant impact on the hydration rate and total porosity of cement paste [21, 22].

Microstructural analysis

Hydrated samples were also prepared at the same w/c ratio of 0.5. The pastes were stored in 10-mL sealed plastic vessels at 20 °C (one vessel for one hydration age). The hydration of the pastes at different ages was stopped by solvent exchange with ethanol for 24 h, and then, the samples were dried in a vacuum-drying oven at 40 °C for 15 min.

The pore size distribution of the hydrated samples was determined by mercury intrusion porosimetry (MIP) at the range of 0.01–10 μm. All the previously dried samples were dried again at 40 °C for 15 min in the vacuum-drying oven before MIP testing.

A part of the dried sample was finely ground to size below 80 μm for powder X-ray diffraction (XRD) analysis. The XRD data were collected on a Rigaku X-ray equipment (Rigaku SmartLab, Cu kα radiation, $\lambda = 0.15406$, the X-ray tube was operated at 40 kV and 35 mA) from 5° to 65° (2θ) at a speed of 5° min^{-1}, with step size of 0.02°.

The finely ground sample was also used for thermogravimetry (TG) and differential scanning calorimetry (DSC), which were performed on Mettler Toledo 1600LF thermal analyzer, and the TG/DSC curves were recorded at a heating rate of 10 °C min^{-1} from 20 °C to 1000 °C in N$_2$ atmosphere.

Small and dried fractured hydrated specimens were used for scanning electron microscopy (SEM) analysis as well. The samples were coated with gold to ensure electrical conductivity.

Results and discussion

Setting time and hydration heat evolution

Setting time

At the normal consistency, setting times for each mix are represented in Table 2 and Fig. 3. It is evident that the water requirement for normal consistency slightly increases with the rise of dose of welan gum. While the value changes from 143 to 156 g as the dose of welan gum goes from 0.00 to 0.25%, the actual solution/cement ratio increases from 0.286 to 0.312, which means that the paste needs higher water to achieve normal consistency with the presence of welan gum. Figure 3 demonstrates the variations of setting times and the differential values between initial and final setting. It is observed that the time period from initial to final setting also increases slightly with the increase in concentration of welan gun. Differences

Table 2 Solution requirement for normal consistency and the corresponding setting time

Concentration of welan gum	Solution requirement for normal consistency^a/g	Setting time/min	
		Initial setting	Final setting
Blank	143	180	226
0.025%	145	189	228
0.05%	146	196	243
0.075%	147	204	252
0.10%	149	209	259
0.25%	156	226	287

^{a} Corresponding to 500 g cement
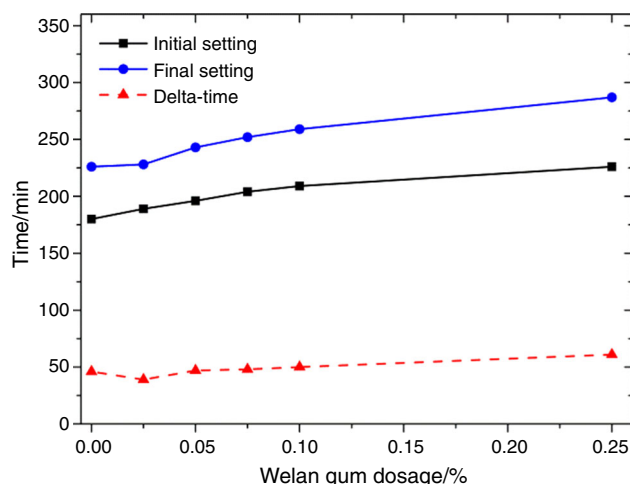
Fig. 3 Initial and final setting time and their difference values variations

(a)

(b)

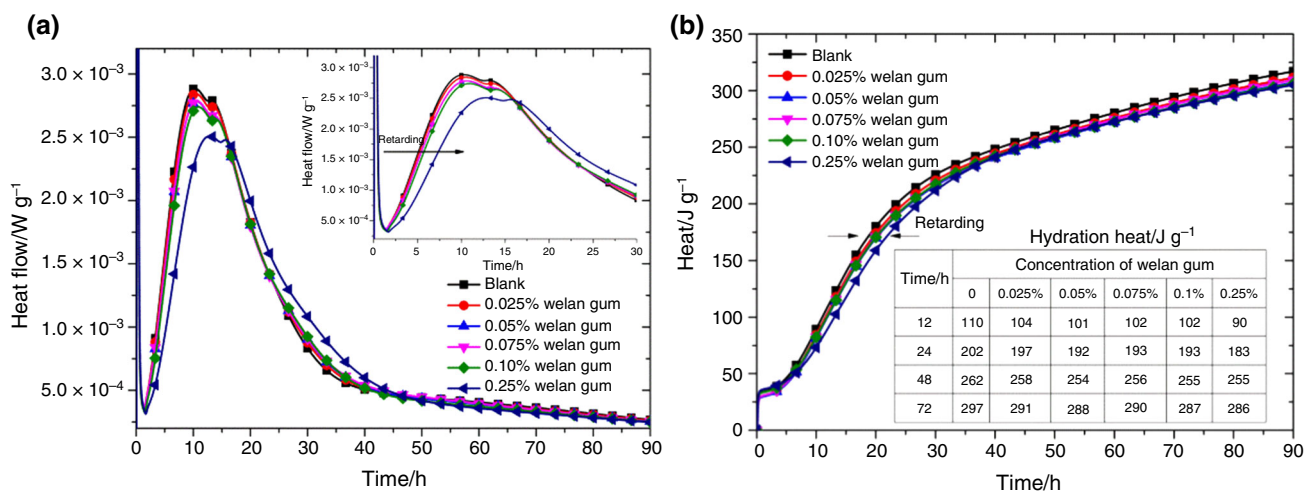|	Hydration heat/J g^{-1}					
Time/h	Concentration of welan gum					
	0	0.025%	0.05%	0.075%	0.1%	0.25%
12	110	104	101	102	102	90
24	202	197	192	193	193	183
48	262	258	254	256	255	255
72	297	291	288	290	287	286

Fig. 4 Calorimetry curves of cement pastes mixed with welan gum. **a** Heat flow rate and **b** cumulative hydration heat

between initial and final setting time also increase slightly with the rise of welan gum. The rising trend of the setting time almost tends to be linear-like trend with the rise of welan gum.

Hydration heat evolution

Figure 4 represents the heat flow (Fig. 4a) and cumulated heat evolution (Fig. 4b) of the six pastes in the first 90 h. Basically, all curves show a similar heat evolution trend. However, it is clear that heat flow at around 15 h, which is attributed to the second hydration of aluminate phase [23], is slightly delayed due to the addition of welan gum (Fig. 4a) and the retarding effect is remarkably observed

when the welan gum dose is 0.25%. The higher the dose of welan gum, the less intensively the reaction of the aluminate phase. Meanwhile, the main hydration peak of C_3S is slightly reduced with the rise of welan gum. Overall, there is a slight retarding effect on the hydration of C_3S and second reaction of the aluminate phase when welan gum dose is less than 0.10% even though the remarkable feature in sample with 0.25%. Combining the evolution of setting time, it is easy to conclude that the setting time of PC is delayed due to the delayed hydration of C_3S and C_3A, which is also correspond to the results of the previous works in the mono-mineral system [19, 20].

The cumulative heat slightly decreases from different 297 to 286 J g^{-1} as the concentration increases from 0.00

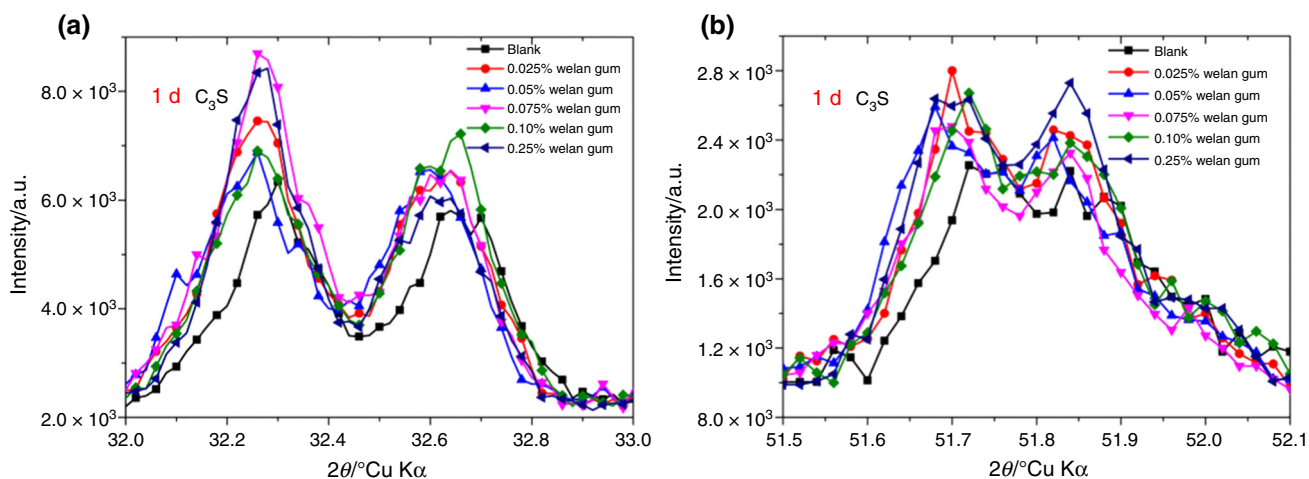Fig. 5 XRD patterns for all the 6 samples with the hydration of 1 d
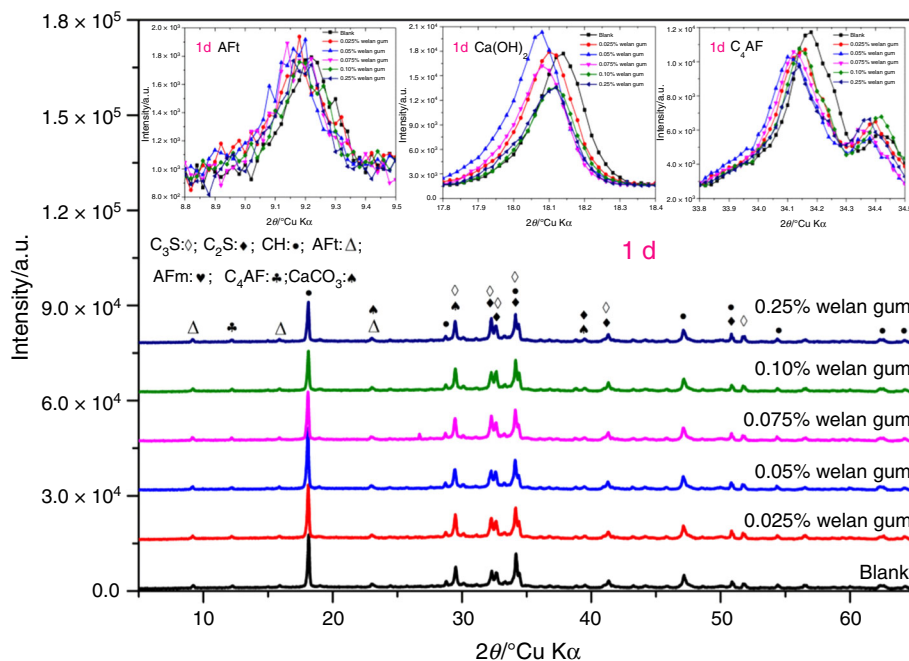
Fig. 6 Portions of XRD patterns of C₃S after hydration for 1 d

to 0.25% welan gum (Fig. 4b). The minor change in heat released in the studied period indicates that welan gum has limited influence on the total heat release of the cement paste.

Hydration products of cement paste

XRD

The XRD patterns of hydrated samples at 1 d are represented in Figs. 5 and 6. Results show the main hydration products in the six samples are very consistent to each other. The AFt contents of the six samples are almost the same; meanwhile, the C_4AF in the five samples is almost the same in the XRD patterns even though there is a little variation of the peak. Figure 6 plots the characteristic diffraction peaks of C_3S. It is clear that the contents of C_3S in specimens with welan gum are a little higher than that in the blank paste, implying the retarding effect of welan gum hydration of C_3S. This is in agreement with the slightly reduced $Ca(OH)_2$ contents in the samples in the presence of welan gum as shown in Fig. 5 and the research of Zhou et al. [20]. The retardation of C_3S can be explained by the variation of Ca^{2+} concentration with or without welan gum: Welan gum decreases Ca^{2+} concentration at early ages and hinders the formation and precipitation of $Ca(OH)_2$. In a word, welan gum affected C_3S early hydration and hindered $Ca(OH)_2$ precipitation on C_3S surface and then influenced the hydration [20].

Figure 7 shows the XRD patterns of selected hydrated cements at different curing ages of 7 and 28 d. Apparently, the content $Ca(OH)_2$ at 7 d is somewhat reduced with the presence of welan gum, but the difference of $Ca(OH)_2$ content is smaller than that in Fig. 6, which means that the retarding effect on C_3S is not obvious at 7 d. Furthermore,

the contents of $Ca(OH)_2$ in the six samples are almost the same to each other at 28 d. Likewise, the contents of C_3S are almost the same at 28 d, even though C_3S is a little retarded within 7 d. Considering the variation of content in C_3S and $Ca(OH)_2$, it is able to find the trend that the addition of welan gum delays the hydration of C_3S at early ages within 7 d; however, the extents of C_3S are almost the same in the six specimens after 28 d.

TG-DSC analysis

TG-DSC analysis was performed to further quantify the hydration products in cement pastes, and the results are shown in Fig. 8, Tables 3 and 4. It is confirmed that the $Ca(OH)_2$ dehydrates at about 400–500 °C and AFt decomposes at around 160 °C from the TG-DSC curves [24–26]. Based on this principle, the contents of $Ca(OH)_2$ and AFt at 28 d of the six mixes are calculated from the mass loss during the heating process. It must be noted that the calculation of the $Ca(OH)_2$ content must exclude C–S–H, who can also lose mass at 400–500 °C. The contents of $Ca(OH)_2$ and AFt of the six samples at different curing ages were calculated and are given in Tables 3 and 4.

It is clear that the contents of $Ca(OH)_2$ are somewhat reduced with the rise of welan gum at 1 d; however, there is no difference of $Ca(OH)_2$ for the six samples at longer curing time. The contents of AFt are relatively constant in all of the six samples at each age. These results are consistent with the XRD results. It suggests that welan gum retards the formation of $Ca(OH)_2$ at very early ages but not AFt.

Furthermore, the degree of hydration (α) can be calculated by Eqs. (1) and (2) with the parameters of dehydroxylation (Ldx), dehydration (Ldh) and decarbonation (Ldc) [27–29], which can be defined according to the
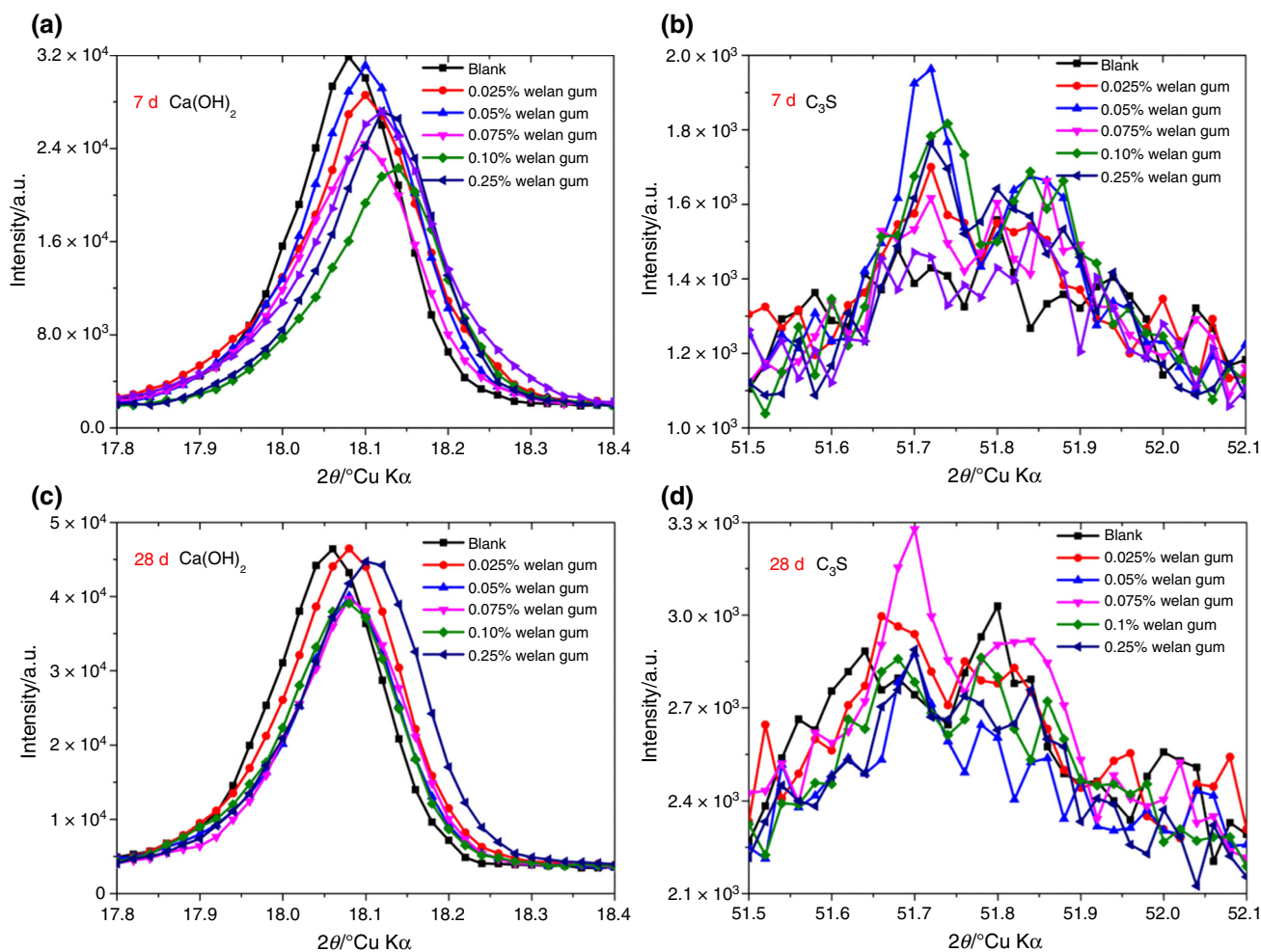
(a)

(b)

(c)

(d)

Fig. 7 XRD patterns for characteristic peaks of $Ca(OH)_2$ and C_3S in selected hydrated cement pastes at 7 day and 28 day
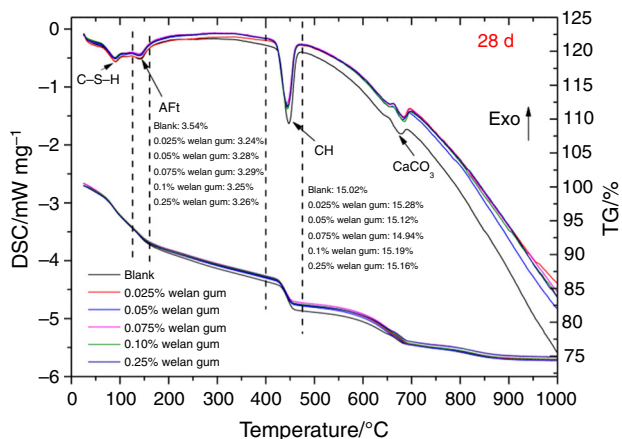

Fig. 8 TG-DSC curves of the 28 d hydrated products of the six samples

Table 3 Contents of $Ca(OH)_2$ (%) of the six samples as determined by TG-DSC

Time/d	1	3	7	28	104
Blank	10.1	13.3	14.1	14.8	15.6
0.025% welan gum	10.2	13.2	14.4	15.3	15.7
0.05% welan gum	10.4	13.2	14.2	15.0	16.3
0.075% welan gum	10.0	13.3	13.8	14.3	15.7
0.10% welan gum	9.9	13.5	14.2	15.2	16.1
0.25% welan gum	9.5	13.3	14.0	14.8	15.9

temperature ranges from the TG-DSC curves. The calculation is based on the amount of chemically bound water (w_B) and the value of 0.41 is a conversion factor and 0.24 represents the maximum amount of chemically bound water required to fully hydrate a cement particle ($w_{B\infty}$). The temperature ranges of Ldx, Ldh and Ldc are shown in Table 5. The degree of hydration of cement pastes confirmed the hydration of cement paste at early ages was a little retarded in the presence (Table 6), while the differences of the degree of hydration were insignificant at longer curing ages, which was corresponded to the results of $Ca(OH)_2$.

Table 4 Contents of AFt (%) of the six samples determined by TG-DSC

Time/d	1	3	7	28	104
Blank	2.0	2.9	3.1	3.5	3.6
0.025% welan gum	2.2	2.7	3.1	3.4	3.6
0.05% welan gum	2.0	2.8	3.1	3.5	3.3
0.075% welan gum	2.0	2.8	3.2	3.5	3.8
0.10% welan gum	2.1	2.9	3.1	3.5	3.2
0.25% welan gum	2.1	2.8	3.1	3.4	3.2

Table 5 Temperature ranges for the different decomposition regions

Region	Temperature range/°C
Ldx	70–400
Ldh	400–500
Ldc	500–750

Table 6 Degree of hydration of the cement pastes at different curing ages (%)

Time/d	1	3	7	28	104
Blank	55.2	68.6	73.7	80.1	84.1
0.025% welan gum	55.2	67.4	73.4	79.7	84.5
0.05% welan gum	54.9	67.1	73.6	79.8	84.1
0.075% welan gum	54.1	66.3	73.2	78.9	83.8
0.10% welan gum	53.6	65.1	72.9	79.1	84.3
0.25% welan gum	52.2	64.3	72.3	78.8	84.0

$$w_B = Ldh + Ldx + 0.41(Ldc) \qquad (1)$$

$$\alpha = \frac{w_B}{0.24} \times 100. \qquad (2)$$

Morphology analysis

SEM images of the 28 d hydrated blank cement paste and cement pastes mixed using 0.05, 0.075 and 0.25% welan gum solutions are shown in Fig. 9. In the samples mixed using the 0.05 and 0.25% welan gum solutions (Fig. 9c, e, f), there are many gel-like particles stick on the hydration products of AFt and C–S–H. In the previous works, researchers [19, 20, 30] assumed that the welan gum are easy to enter the hydration products and slow the nucleation of hydration products such as AFt and Ca(OH); simultaneously, welan gum are easy to form three-dimensional network when sear is removed. Herein, the gel-like particles are highly possible to be welan gum, but that needs more work to verify. In addition, the microstructures of the hydrated cement pastes with higher doses of welan gum (Fig. 9d, e) are more porous than the blank sample. More welan gum takes up the space of the hydration products, which can result a higher porosity in paste with higher dose of welan gum. The shapes of the AFt phase (Fig. 9b, d, e) in the images are similar, which means that the use of welan gum in cement pastes does not change the morphology of AFt phase in Portland cement.
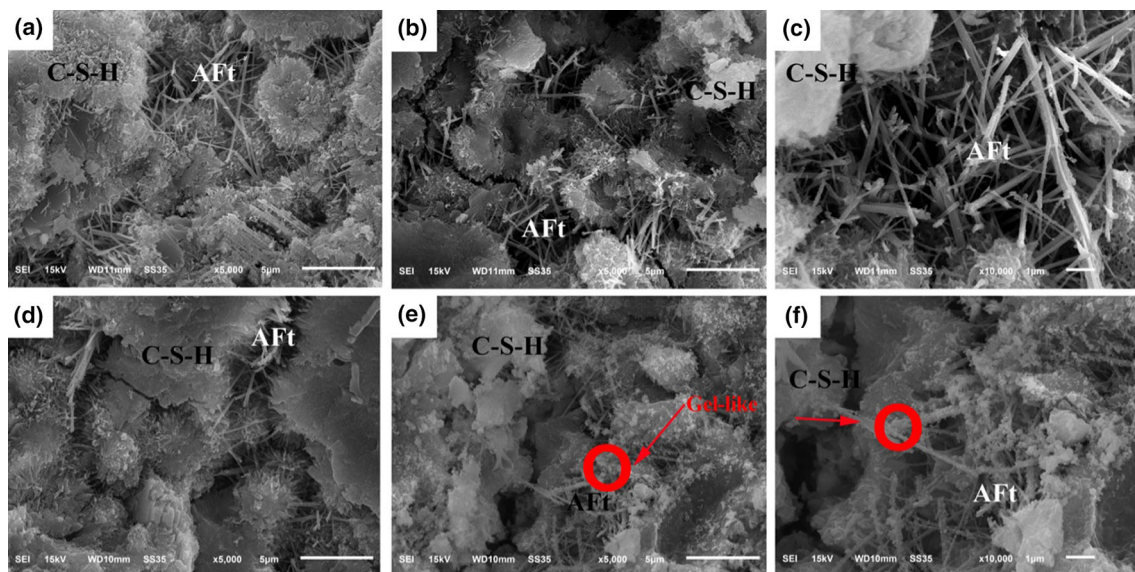
Fig. 9 SEM images of cement pastes at 28 d. **a** Blank cement paste; **b, c** mixed with 0.05% welan gum solution; **d** mixed with 0.075% welan gum solution; **e, f** mixed with 0.25% welan gum solution
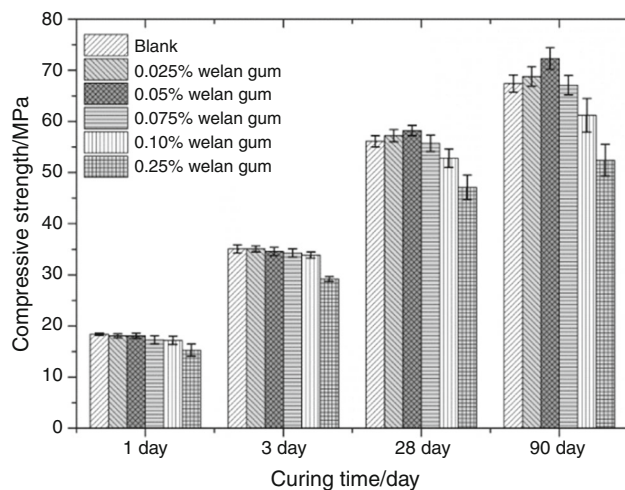
Fig. 10 Compressive strengths evolution of cement mortars with welan gum

Compressive strength and microstructure

Compressive strength

The compressive strengths of the six specimens at 1, 3, 28 and 90 d are presented in Fig. 10. Result shows that compressive strength of the cement mortar increases with curing time; the addition of welan gum has different influences on the compressive strength development. At early ages of 1 and 3 d, the compressive strengths of samples are almost the same in the presence of different dose of welan gum. This trend is in agreement with the setting time and the hydration evolution as determined by calorimetry. After 28 d, compressive strength exhibits certain growth when the concentration of welan gum is lower than 0.05% and such a trend goes to sharper at 90 d. When samples mixed with welan gum higher than 0.075%, the compressive strengths of samples at each age are lower than that of control sample. Overall, the compressive strength at longer curing times is significantly lower than the blank when the dose of welan gum exceeds 0.10%.

Pore size distribution and porosity

The pore size distribution and cumulative volumes for hydrated cement pastes at 1, 3 and 28 d are illustrated in Fig. 11 and Table 7. In the first day (Fig. 11a), the pore size and volume both increase with the rise of welan gum showing as the increase in larger pores in the pastes with welan gum, which confirms the retarding effect of welan gum on the hydration of C_3S at 1 d. Meanwhile, the sample mixed with 0.05% welan gum has the similar pore cumulative volumes with the controlled sample. As the curing time increases (Table 7; Fig. 11b, c), the pores all shift to
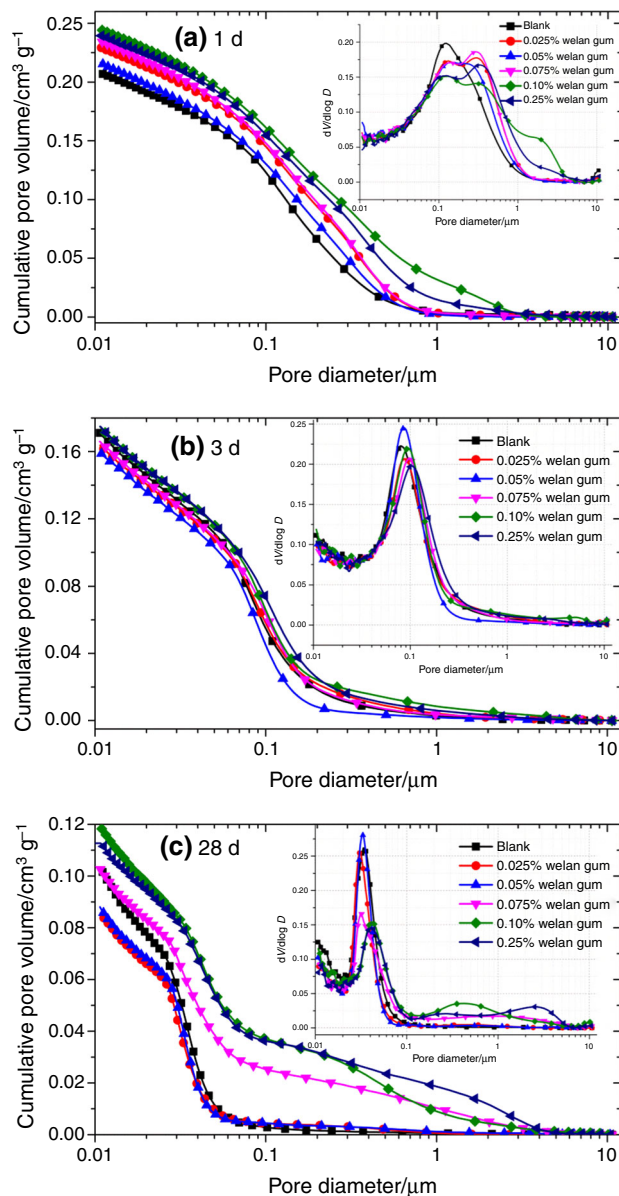

Fig. 11 Pore size distribution and accumulation of the cement pastes with welan gum at **a** 1 d, **b** 3 d and **c** 28 d

Table 7 Total porosity of cement pastes at curing ages of 1, 3 and 28 d

Sample	Total porosity/%		
	1 d	3 d	28 d
Blank	20.78	16.38	10.16
0.025% welan gum	22.95	15.98	8.38
0.05% welan gum	21.57	15.68	8.34
0.075% welan gum	23.26	16.55	10.75
0.10% welan gum	24.45	17.49	11.58
0.25% welan gum	23.97	17.46	11.15

smaller region and the cumulative volumes are also decreased. This is a good explanation of the development of compressive strength of the samples that the pore volume is reduced and even less than the control one with the curing time extends. At 28 d, cement pastes with welan gum below 0.075% have lower porosity than that in blank, while samples with welan gum higher than 0.075% have more macropores. In particular, the paste with 0.05% welan gum has the least porosity among all the samples, which is correspondent to the highest compressive strength over 28 d, while samples with higher porosity seem to have lower compressive strengths. The relationship between porosity (by MIP) and compressive strength was reported well in previous study [31, 32]. Combining the results of XRD, TG-DSC and SEM, it is easy to conclude that although welan gum does not change the morphology of the hydration products of cement pastes, it promotes the development compressive strength and porosity of mortars with welan gum lower than 0.075%.

Conclusions

Based on the above results and discussions, the following conclusions can be drawn with the effects of welan gum dosage on the hydration of PC.

1. The water requirement for normal consistency increases with the rise of welan gum; owning to the retarding effect of welan gum on C_3A and C_3S, the setting time of cement paste is prolonged by welan gum and such an effect tends to be more obvious with the rise of welan gum.

2. Welan gum delays the induction period and the second reaction of the aluminate phase, but has very limited influence on the total heat release of cement paste. The hydration of C_3S is a little retarded at early hydration time; meanwhile, welan gum affects the formation of $Ca(OH)_2$ but not AFt.

3. From the SEM analysis, welan gum does not affect the morphologies of hydration products, but there are many gel-like particles stick on the surface of the hydration product, which can be a reason for the higher porosity in hardened cement pastes with high dose of welan gum.

4. The use of 0.05% welan gum solution promotes the compressive strength development at longer ages and reduces the pore size of the cement paste. The higher porosity of hardened cement pastes with higher dose of welan gum results in the decreased compressive strength. Overall, cement paste with 0.05% welan gum shows good performances in long-term compressive strength development and porosity.

References

1. Khayat KH. Viscosity-enhancing admixtures for cement-based materials—an overview. Cem Concr Compos. 1998;20:171–88.
2. Plank J. Applications of biopolymers and other biotechnological products in building materials. Appl Microbiol Biotechnol. 2004;66:1–9.
3. Kaur V, Bera MB, Panesar PS, Kumar H, Kennedy JF. Welan gum: microbial production, characterization, and applications. Int J Biol Macromol. 2014;65:454–61.
4. Paniagua-Michel JdJ, Olmos-Soto J, Morales-Guerrero ER. Chapter eleven—algal and microbial exopolysaccharides: new insights as biosurfactants and bioemulsifiers. In: Se-Kwon K, editor. Advances in food and nutrition research. London: Academic Press; 2014. p. 221–57.
5. Zhu P, Dong S, Li S, Xu X, Xu H. Improvement of welan gum biosynthesis and transcriptional analysis of the genes responding to enhanced oxygen transfer by oxygen vectors in Sphingomonas sp. Biochem Eng J. 2014;90:264–71.
6. Khayat KH. Frost durability of concrete containing viscosity-modifying admixtures. ACI Mater J. 1995;92:625–33.
7. Khayat KH. Effects of antiwashout admixtures on properties of hardened concrete. ACI Mater J. 1996;93:134–46.
8. Lachemi M, Hossain KMA, Lambros V, Nkinamubanzi PC, Bouzoubaâ N. Performance of new viscosity modifying admixtures in enhancing the rheological properties of cement paste. Cem Concr Res. 2004;34:185–93.
9. Khayat KH, Ballivy G, Gaudreault M. High-performance cement grout for underwater crack injection. Can J Civ Eng. 1997;24:405–18.
10. Khayat KH, Yahia A. Effect of welan gum high-range water reducer combinations on rheology of cement grout. ACI Mater J. 1997;94:365–72.
11. Khayat KH, Sonebi M. Effect of mixture composition on washout resistance of highly flowable underwater concrete. ACI Mater J. 2001;98:289–95.
12. Sonebi M. Rheological properties of grouts with viscosity modifying agents as diutan gum and welan gum incorporating pulverised fly ash. Cem Concr Res. 2006;36:1609–18.
13. Sonebi M, Khayat KH. Effect of water velocity on performance of underwater self-consolidating concrete. ACI Mater J. 1999;96:519–28.
14. Isik IE, Ozkul MH. Utilization of polysaccharides as viscosity modifying agent in self-compacting concrete. Constr Build Mater. 2014;72:239–47.
15. Crescenzi V, Dentini M, Coviello T, Rizzo R. Comparative analysis of the behavior of gellan gum (S-60) and welan gum (S-130) in dilute aqueous solution. Carbohyd Res. 1986;149:425–32.
16. Lopes L, Milas M, Rinaudo M. Influence of the method of purification on some solution properties of welan gum. Int J Biol Macromol. 1994;16:253–8.
17. Rols S, Ambroise J, Péra J. Effects of different viscosity agents on the properties of self-leveling concrete. Cem Concr Res. 1999;29:261–6.

18. Łaźniewska-Piekarczyk B. The type of air-entraining and viscosity modifying admixtures and porosity and frost durability of high performance self-compacting concrete. Constr Build Mater. 2013;40:659–71.

19. Ma L, Zhao Q, Yao C, Zhou M. Impact of welan gum on tricalcium aluminate–gypsum hydration. Mater Charact. 2012;64: 88–95.

20. Zhang Y, Liu C, Luping Z, Qu C, Zhao Q. The impact of welan gum on C_3S hydration system. In: Proceedings of the 15th ICCC, 2; 2015. p. 353.

21. Atahan HN, Oktar ON, Taşdemir MA. Effects of water–cement ratio and curing time on the critical pore width of hardened cement paste. Constr Build Mater. 2009;23:1196–200.

22. Ma B, Ma M, Shen X, Li X, Wu X. Compatibility between a polycarboxylate superplasticizer and the belite-rich sulfoaluminate cement: setting time and the hydration properties. Constr Build Mater. 2014;51:47–54.

23. Taylor HFW. Cement chemistry. London: Thomas Telford; 1997.

24. Lothenbach B, Winnefeld F. Thermodynamic modelling of the hydration of Portland cement. Cem Concr Res. 2006;36:209–26.

25. Michel M, Georgin J-F, Ambroise J, Péra J. The influence of gypsum ratio on the mechanical performance of slag cement accelerated by calcium sulfoaluminate cement. Constr Build Mater. 2011;25:1298–304.

26. Soin AV, Catalan LJJ, Kinrade SD. A combined QXRD/TG method to quantify the phase composition of hydrated Portland cements. Cem Concr Res. 2013;48:17–24.

27. Pane I, Hansen W. Investigation of blended cement hydration by isothermal calorimetry and thermal analysis. Cem Concr Res. 2005;35:1155–64.

28. Monteagudo SM, Moragues A, Gálvez JC, Casati MJ, Reyes E. The degree of hydration assessment of blended cement pastes by differential thermal and thermogravimetric analysis. Morphological evolution of the solid phases. Thermochim Acta. 2014;592:37–51.

29. Xu Z, Li W, Sun J, Hu Y, Xu K, Ma S, Shen X. Research on cement hydration and hardening with different alkanolamines. Constr Build Mater. 2017;141:296–306.

30. Zhang Y, Zhao Q, Liu C, Zhou M. Properties comparison of mortars with welan gum or cellulose ether. Constr Build Mater. 2016;102:648–53.

31. Ramezanianpour AM, Hooton RD. A study on hydration, compressive strength, and porosity of Portland-limestone cement mixes containing SCMs. Cem Concr Compos. 2014;51:1–13.

32. Queiroz VMS, Fontes SR. Experimental analysis of structural change and rheological behavior of macromolecular solutions with guar and xanthan gums in crossflow microfiltration processing. Food Bioprocess Technol. 2008;1:180–6.